

Cosmic Rays from Dark Matter Annihilation and Big-Bang Nucleosynthesis

Junji Hisano^(a,b), Masahiro Kawasaki^(a,b), Kazunori Kohri^(c), Takeo Moroi^(b,d) and
Kazunori Nakayama^(a)

^a*Institute for Cosmic Ray Research, University of Tokyo, Kashiwa 277-8582, Japan*

^b*Institute for the Physics and Mathematics of the Universe, University of Tokyo,
Kashiwa 277-8568, Japan*

^c*Physics Department, Lancaster University, Lancaster LA1 4YB, UK*

^d*Department of Physics, Tohoku University, Sendai 980-8578, Japan*

Abstract

Recent measurements of cosmic-ray electron and positron fluxes by PAMELA and ATIC experiments may indicate the existence of annihilating dark matter with large annihilation cross section. We show that the dark matter annihilation in the big-bang nucleosynthesis epoch affects the light element abundances, and it gives stringent constraints on such annihilating dark matter scenarios for the case of hadronic annihilation. Constraints on leptonically annihilating dark matter models are less severer.

1 Introduction

Cosmological observations have revealed that about 20 percent of the total energy density of the Universe is dominated by the dark matter (DM) [1], whose detailed properties are still unknown, and many physicists believe that the DM is a kind of stable particle appearing in the physics beyond the standard model. Thus, to determine the origin and nature of the dark matter in the Universe is one of the most important topics in the particle physics, and some methods were proposed for detecting the signals of the DM directly or indirectly [2, 3]. One of such methods is that to search for high-energy cosmic-rays, including gamma-rays, positrons, anti-protons and neutrinos, which come from the DM annihilation in our Galaxy.

Recent results of the cosmic-ray positron and electron fluxes by the PAMELA satellite experiment [4] and the ATIC balloon experiment [5] are now drawing a lot of attention, since the steep excess observed by these experiments can be interpreted as an extra contribution from the DM annihilation. (For earlier papers, see [6].) However, in order to explain these signals the annihilation cross section should be fairly large, as $\langle\sigma v\rangle \sim (10^{-24} - 10^{-23}) \text{ cm}^3\text{s}^{-1}$, which may be achieved by the Sommerfeld enhancement effect [7]. This is orders of magnitude larger than the standard value $\langle\sigma v\rangle \sim 3 \times 10^{-26} \text{ cm}^3\text{s}^{-1}$, which reproduces the observed DM abundance under the thermal freezeout scenario [2]. Then, a huge boost factor ($B_F \sim 100$), which is due to the enhancement of the DM annihilation rate due to the clumpy structure of the DM halo, should be introduced in the scenario if $\langle\sigma v\rangle$ is not varied in time. However, the DM may be produced nonthermally in other ways, such as late-decay of long lived particles [8, 9]. Once we give up the thermal freezeout scenario, a large annihilation cross section is still allowed.

The DM with large annihilation rate leads to other observable signatures: gamma-rays, anti-protons, and neutrinos.¹ In particular, even if the DM only annihilates into leptons, the internal bremsstrahlung processes always emit significant amount of gamma-rays, and it also predicts a comparable amount of neutrinos. Those may put stringent constraints on the DM models [11, 12].

Besides these cosmic-ray signals, in this paper we show that the DM annihilation also affects the prediction of the big-bang nucleosynthesis (BBN), since it injects high-energy particles in the nucleosynthesis epoch, which modify the light elements abundances. Such an effect of DM annihilation was pointed out by Jedamzik in Ref. [13], where the modification on the ${}^6\text{Li}$ abundance due to the hadronic process was emphasized. (See also Refs. [14, 15] for early studies of DM annihilation effects on BBN.) This subject was recently studied by four of the present authors in connection with the observed positron excess [16]. In this paper we have performed more systematic studies on the effect of DM annihilation on BBN, including the case where the DM annihilates into only leptons, motivated by recent results of PAMELA/ATIC. In such a case, the photo-dissociations of light elements give constraint. In particular, we found that the ${}^3\text{He}$ to D ratio gives the most stringent constraint on the annihilation cross section, which can be consistent

¹Indirect detection signatures of non-thermally produced DM were investigated in Ref. [10] before PAMELA and ATIC.

with the PAMELA/ATIC results. We also consider the case that the DM annihilates into hadrons. Then, the BBN constraint becomes more stringent, and a boost factor larger than unity must be introduced in order to account for the PAMELA/ATIC anomalies. Therefore, the DM annihilation models as an explanation of the PAMELA/ATIC results should be treated carefully so as not to contradict with the BBN constraint presented in this paper.

This paper is organized as follows. In Sec. 2 effects of DM annihilation on BBN are explained both for the cases of radiative and hadronic annihilation modes. Current status of observations of light element abundances is summarized there. In Sec. 3 the resultant constraints on the DM annihilation cross section and also their implications to the PAMELA/ATIC observations are presented. Sec. 4 is devoted to conclusions and discussion.

2 BBN with Annihilating Dark Matter

2.1 Light element abundances: theory

As discussed in the introduction, we consider the BBN scenario with DM particle which has sizable annihilation cross section. In such a scenario, the annihilation rate of the DM during the BBN epoch may be significant and the abundances of the light elements may be affected by energetic particles emitted via the annihilation process.

For the study of the effects of the DM annihilation during BBN epoch, it is necessary to calculate the production rate of energetic particles (i.e., γ , e^\pm , hadrons, and so on) via the annihilation. Denoting the pair annihilation cross section of the DM as $\langle\sigma v\rangle$, the production rate of the energetic particle I is given by

$$\left[\frac{df_I}{dt}\right]_{\text{ann}} = \frac{1}{2}n_{\text{DM}}^2\langle\sigma v\rangle \left[\frac{dN_I}{dE}\right]_{\text{ann}}, \quad (1)$$

where $f_I(E, t)$ is the energy spectrum of the particle I at a time t , and $[dN_I/dE]_{\text{ann}}$ is the energy distribution of I from the single annihilation process. In our study, we assume that the pair annihilation is dominantly via s -wave processes, and that $\langle\sigma v\rangle$ is independent of time.

In addition, n_{DM} is the DM number density (at the time t), which is given by

$$n_{\text{DM}} = \frac{\Omega_{\text{DM}}\rho_{\text{crit}}}{m_{\text{DM}}} \left(\frac{a_0}{a(t)}\right)^3, \quad (2)$$

where ρ_{crit} is the present critical density, m_{DM} is the DM particle mass, and a_0 and $a(t)$ are the scale factors at present and at the time t , respectively. For the density parameter for the DM, we take $\Omega_{\text{DM}} = 0.206$ [1]. The energy distribution $[dN_I/dE]_{\text{ann}}$ strongly depends on the properties of the DM; it is sensitive to how the DM annihilates. In particular, if quarks and/or gluon are produced via the annihilation, we should take account of the

Final State	$E_{\text{vis}}/m_{\text{DM}}$
e^+e^-	2.00
$\mu^+\mu^-$	0.70
$\tau^+\tau^-$	0.62
W^+W^-	0.94

Table 1: Visible energy carried by e^\pm s and photons after annihilation and subsequent decay, E_{vis} , in single DM annihilation process.

hadronization process in calculating $[dN_I/dE]_{\text{ann}}$. We use the PYTHIA package [18] for the precise estimation of the distribution functions.

It should be noted that, as one can see from Eq. (1), the production rate of the energetic particles (per one DM particle), which is given by $\sim n_{\text{DM}}\langle\sigma v\rangle$, is proportional to a^{-3} and is enhanced in the early Universe. This is a significant contrast to the case where the DM particle is unstable. The PAMELA and ATIC anomalies can be explained if the present production rate of e^\pm is $\sim 10^{-26} \text{ s}^{-1}$, which may be realized either by the annihilation or the decay. If the production of e^\pm is via the decay, the production rate is given by the decay rate of the DM particle and is a constant of time. Then, the production rate of the energetic particles is too small during the BBN epoch to affect the abundance of light elements.

Effects of the DM annihilation is classified into (i) photo-dissociation, and (ii) $p \leftrightarrow n$ conversion due to emitted pions and hadro-dissociation. In the following, we summarize important points in these effects.

2.1.1 Photo-dissociation of light elements

The high energy charged leptons and photons emitted into the cosmic plasma induce electromagnetic showers and produce copious energetic photons. These photons destroy the light elements (^4He , ^3He , D and ^7Li) synthesized in BBN through photo-dissociate processes [19, 20].

The effect of photo-dissociation is determined only by the amount of total visible energy E_{vis} of produced particles in the annihilation if $E_{\text{vis}} \gg 10 \text{ MeV}$ [19]. Here “visible energy” is defined by the sum of energies carried by e^\pm s and photons after annihilation and subsequent decay. Importantly, E_{vis} depends on the annihilation modes of dark matter. We estimate E_{vis} using the PYTHIA package; for the final states which will be studied in the following, we show the ratio $E_{\text{vis}}/m_{\text{DM}}$ in Table 1. (Notice that the ratio $E_{\text{vis}}/m_{\text{DM}}$ is independent of m_{DM} once the final state is fixed. In addition, $E_{\text{vis}} \leq 2m_{\text{DM}}$ because we consider pair annihilation processes of the DM.)

Once E_{vis} is given, the rate of the visible energy injection during the BBN epoch is given by

$$\left[\frac{d\rho_{\text{vis}}}{dt}\right]_{\text{ann}} = \frac{1}{2}E_{\text{vis}}n_{\text{DM}}^2\langle\sigma v\rangle. \quad (3)$$

With the given injection rate, the spectra of the energetic photon and electron induced by the DM annihilation are obtained by solving a set of Boltzmann equations, which include effects of various radiative processes (photon-photon pair creation, inverse Compton scattering, Thomson scattering and so on). Then, we have incorporated the photo-dissociation rates in network calculation of BBN and obtained the abundances of the light elements. In this calculation we have used the most recent data for nuclear reaction rates [21, 22, 23, 24, 25] and estimated the theoretical errors by Monte Carlo method [26, 21].

The details of the photo-dissociation effects have been discussed, for example, in Ref. [20]. The important points of the photo-dissociation effects are summarized as follows:

- $T \gtrsim 10$ keV: The emitted high energy photons are quickly thermalized through photon-photon process and no significant photo-dissociation of the light elements occurs.
- $1 \text{ keV} \lesssim T \lesssim 10 \text{ keV}$: The only D is destroyed by the high energy photons and its abundance decreases. The other light elements are not affected.
- $T \lesssim 1$ keV: All light elements are destroyed by the high energy photons produced by DM annihilation. As a result, the abundance of ${}^4\text{He}$ decreases while D, ${}^3\text{He}$ and ${}^6\text{Li}$ are non-thermally produced. In this case ${}^3\text{He}$ to D ratio gives the most stringent constraint.

Here we make comments on annihilation onto hadronic particles. Even if DM annihilates mainly into charged leptons, we expect some emission modes into hadrons via, for example, $\text{DM} + \text{DM} \rightarrow \ell^+ + \ell^- + Z^*$, where ℓ^\pm denotes charged lepton hereafter. As will be seen in next subsection, energetic hadrons, especially nucleons, cause “hadro-dissociation” of the light elements and give more serious effect on BBN than high energy electrons and photons [27, 28, 29, 30, 31]. However, the expected branching ratio into hadrons is $\sim 10^{-3}$, which is too small to give a significant constraint in the present problem. (See Fig. 3.)

For annihilation into τ 's, pions are produced from τ decays. Approximately 0.9 charged pions are emitted by the decay of τ lepton in average. As we will see in the next section, the effect of pions might be important at around $T \sim 1$ MeV when the n/p is affected by $n + \pi^+ \rightarrow p + \pi^0$ and $p + \pi^- \rightarrow n + \pi^0$. The $p \leftrightarrow n$ inter-converting reactions increase n/p , which results in larger value of the ${}^4\text{He}$ abundance. However, we have checked that the constraint from the overproduction of ${}^4\text{He}$ is much weaker than the constraint from the photo-dissociation.

2.1.2 Hadronic effects

Next we discuss the effects of hadron emissions on the abundances of the light elements. As we will see, if the annihilation process has a hadron-emission mode with a net branching ratio of $\gtrsim \text{O}(10)\%$, the most stringent constraint is mainly from the hadronic modes. The exceptional case is that the emission time is very late ($T \lesssim 0.3$ keV).

Once energetic colored particles are emitted by the annihilation, they are hadronized and the energetic mesons and baryons are produced. In particular, once energetic nucleons are emitted after the hadronization process, they may scatter off the background nuclei and induce non-thermal production and destruction processes of light elements. The most significant processes are via the scattering off the background ${}^4\text{He}$. The effects of the non-thermal production of the nuclei A ($= \text{D}, {}^3\text{He}, {}^4\text{He}, {}^6\text{Li}, \text{and } {}^7\text{Li}$) can be taken into account by including the following production term into the Boltzmann equations:

$$\left[\frac{dn_A}{dt} \right]_{\text{ann}} = \frac{1}{2} \xi_{A,\text{ann}} n_{\text{DM}}^2 \langle \sigma v \rangle. \quad (4)$$

Here, $\xi_{A,\text{ann}}$ is the number of the produced nucleus A per single annihilation process, which depends on the background temperature and the energy spectrum of the emitted hadrons. The spectra of the produced hadrons depend on the annihilation mode and the mass of the DM. We note here that the mass-dependence is given by $\xi_{A,\text{ann}} \propto m_{\text{DM}}^{0.5 \pm \delta}$ with $\delta \lesssim 0.2$ [29]. Then, as we see in the following, the constraint from the hadron emission approximately scales as $\propto \langle \sigma v \rangle / m_{\text{DM}}^{1.5}$. Such processes become effective when the cosmic temperature is lower than ~ 0.1 MeV.

At higher cosmic temperature, another process, which is the $p \leftrightarrow n$ conversion process induced by emitted pions, is more effective. If the cosmic temperature is sufficiently high ($T \gtrsim 0.1$ MeV), all the emitted hadrons are stopped through electromagnetic interaction with background electrons and photons before they scatter off the background nuclei. In that case, the stopped hadrons such as charged pions (as well as $n\bar{n}$ and $p\bar{p}$) scatters off the background nuclei only through exothermic reactions with their threshold cross sections. Then background neutron and proton are inter-converted each other through the process like $n + \pi^+ \rightarrow p + \pi^0$ and $p + \pi^- \rightarrow n + \pi^0$. Those processes change the neutron to proton ratio even after the freezeout time of neutron. In this case more ${}^4\text{He}$ and D are produced through the non-thermal interconversion processes [14, 32]. Note that unstable hadrons such as π^0 decay with short lifetimes ($\tau \ll 10^{-8}$ sec) and disappear well before contributing to the inter-converting process.

We have included the relevant hadro-dissociation processes as well as effects of $p \leftrightarrow n$ conversion into the BBN network calculation and obtained the light element abundances. The details are discussed in [28, 29, 30], and here we just summarize the most important features of the hadronic effects:

- $T \gtrsim 10$ MeV: The emitted hadrons cannot change the neutron to proton ratio and do not affect any light element abundances at all.
- $100 \text{ keV} \lesssim T \lesssim 10 \text{ MeV}$: ${}^4\text{He}$ and D are produced through the $n \leftrightarrow p$ interconversion caused by stopped mesons (π^\pm) and/or nucleon-antinucleon pairs ($p\bar{p}$ and $n\bar{n}$).
- $10 \text{ keV} \lesssim T \lesssim 100 \text{ keV}$: ${}^4\text{He}$ is destroyed by energetic nucleons. That produces a lot of energetic D, T and ${}^3\text{He}$. Among those daughter nuclei, D gives most stringent bounds on the amount of the primary nucleons emitted by the annihilation.

- $0.3 \text{ keV} \lesssim T \lesssim 10 \text{ keV}$: ${}^6\text{Li}$ is non-thermally produced by the scattering between the background ${}^4\text{He}$ and the energetic T. This gives the severest bound.
- $T \lesssim 0.3 \text{ keV}$: The effect from the photo-dissociation can dominate and the ${}^3\text{He}$ to D ratio gives the severest bound when $E_{\text{vis}}/m_{\text{DM}} \gtrsim 0.1$ even if the hadronic mode is at 100%.

2.2 Light element abundances: observations

Next, we summarize observational constants on primordial abundances of D, ${}^3\text{He}$, ${}^4\text{He}$, ${}^6\text{Li}$ and ${}^7\text{Li}$, which we adopt in our study. The errors are presented at 1σ . The subscript “p” and “obs” are for the primordial and observational values, respectively.

The primordial value of D abundance is inferred from observation of high redshift QSO absorption systems. We adopt a following observational constraints on the deuterium abundance as “Low” value:

$$\text{Low } (n_{\text{D}}/n_{\text{H}})_{\text{p}} = (2.82 \pm 0.26) \times 10^{-5}, \quad (5)$$

which is the most-recently reported value derived by taking the weighted mean of six observed QSO absorption systems [33]. This value well agrees with the baryon to photon ratio suggested by the WMAP 5-year CMB anisotropy observation [1]. However, the six measurements have a larger dispersion as expected. In addition, the deuterium is the most fragile element. So, in order to derive a conservative constraint, we also adopt the highest value among the six measurements as “High” D/H,

$$\text{High } (n_{\text{D}}/n_{\text{H}})_{\text{p}} = (3.98_{-0.67}^{+0.59}) \times 10^{-5}. \quad (6)$$

To constrain the primordial ${}^3\text{He}$ abundance, we use an observational ${}^3\text{He}$ to D ratio as an upper bound, which is a monotonically increasing function of the cosmic time. (For details, see Refs. [34, 29].) In this study we adopt the newest values of D and ${}^3\text{He}$ abundances simultaneously observed in protosolar clouds (PSCs), $(n_{{}^3\text{He}}/n_{\text{H}})_{\text{PSC}} = (1.66 \pm 0.06) \times 10^{-5}$ and $(n_{\text{D}}/n_{\text{H}})_{\text{PSC}} = (2.00 \pm 0.35) \times 10^{-5}$ [35]. Then we get

$$(n_{{}^3\text{He}}/n_{\text{D}})_{\text{p}} < 0.83 + 0.27. \quad (7)$$

The mass fraction of ${}^4\text{He}$ is determined by the measurement of recombination lines from extragalactic HII regions. In the most recent analysis [36], two values are reported by using old and new ${}^4\text{He}$ -emissivity data, $Y_{\text{p}} = 0.2472 \pm 0.0012$ and $Y_{\text{p}} = 0.2516 \pm 0.0011$, respectively. Notice that the error presented in [36] does not include systematic effects. Thus, in this study, we add an error of 0.0040 [37] to derive conservative constraint:

$$Y_{\text{p}} = 0.2516 \pm 0.0040. \quad (8)$$

(For the systematic uncertainty of the observed ${}^4\text{He}$ abundance, see also Ref. [38].)

For ${}^7\text{Li}$ observed abundance in high temperature metal-poor population II stars is considered as primordial. Here, we adopt the most recent value of the ${}^7\text{Li}$ to hydrogen

ratio $\log_{10}({}^7\text{Li}/\text{H})_{\text{obs}} = -9.90 \pm 0.09$ given in Ref. [39]. This is close to the value given in Ref. [40]: $\log_{10}({}^7\text{Li}/\text{H})_{\text{obs}} = -9.91 \pm 0.10$. On the other hand, a slightly larger value has been also reported in Ref. [41]: $\log_{10}({}^7\text{Li}/\text{H})_{\text{obs}} = -9.63 \pm 0.06$. The problem is that the theoretical value of ${}^7\text{Li}$ is much larger than the observational one even if we adopt the higher value of the observational abundance. The situation becomes worse when we use an updated reaction rate of ${}^4\text{He}({}^3\text{He}, \gamma){}^7\text{Be}$ [25, 42]. The observational values in Refs. [39] and [41] are smaller than the standard BBN prediction by approximately 0.35 dex and 0.25 dex, respectively. As for ${}^6\text{Li}$ abundance, on the other hand, recent observation shows that the theoretical value is much smaller than that of the observation, $({}^6\text{Li}/{}^7\text{Li})_{\text{obs}} = 0.046 \pm 0.022$ [43]. These two discrepancies may be collectively called “lithium problem”. Concerning the inconsistency between the face value of the primordial ${}^7\text{Li}$ abundance and the standard BBN prediction, various solutions have been discussed from the viewpoints of both astrophysics [44, 45, 46] and cosmology [47, 27, 31].² However, the main purpose of this paper is to derive a conservative constraint, so we do not go into the details of these models. Instead, assuming some depletion, we add an additional systematic error of +0.35 dex into the observational face value $n_{7\text{Li}}/n_{\text{H}}$ in our study:

$$\log_{10}(n_{7\text{Li}}/n_{\text{H}})_p = -9.90 \pm 0.09 + 0.35. \quad (9)$$

Notice that this depletion factor $D_7 = 0.35$ is the systematic error a little larger than that allowed from effect of ${}^7\text{Li}$ depletion by rotational mixing in stars [44].³

As for a ${}^6\text{Li}$ constraint, we use $(n_{6\text{Li}}/n_{7\text{Li}})_{\text{obs}} = 0.046 \pm 0.022$, which was newly-observed in a very metal-poor star [43]. We also add a systematic error of +0.106 [50] to take into account depletion effects in stars adopting the relation between ${}^7\text{Li}$ and ${}^6\text{Li}$ depletion factors, $D_6 = 2.5D_7$ [51, 44],⁴ which leads to $\Delta \log_{10}(n_{6\text{Li}}/n_{7\text{Li}}) = 0.525$ for $D_7 = 0.35$. Then we get a following upper bound:

$$(n_{6\text{Li}}/n_{7\text{Li}})_p < 0.046 \pm 0.022 + 0.106. \quad (10)$$

3 Constraints on Annihilation Cross Section

Now, we show the constraints on the annihilation cross section of the DM particle. As shown in Eq. (1), the amount of energetic particles produced by the annihilation process is proportional to the annihilation cross section, and hence the effects on the light element abundances become more enhanced as the cross section becomes larger. Since the light

²For references, see also [48] for possible astrophysical scenarios to enhance ${}^6\text{Li}$ abundance, and [49] for its observational uncertainties.

³The depletion factor D_7 is defined as $D_7 = \Delta \log_{10}({}^7\text{Li}/\text{H})$. The depletion factor for ${}^6\text{Li}$ is defined similarly.

⁴This relation is obtained for depletion by rotational mixing. If the depletion is caused by atomic diffusion [45], this relation is no longer correct. Instead we should have used $D_6 \simeq D_7$. However, in this case the upper bound on ${}^6\text{Li}/{}^7\text{Li}$ becomes more stringent than given by Eq. (10). We prefer to use the relation for the rotation mixing because we will get more conservative constraint.

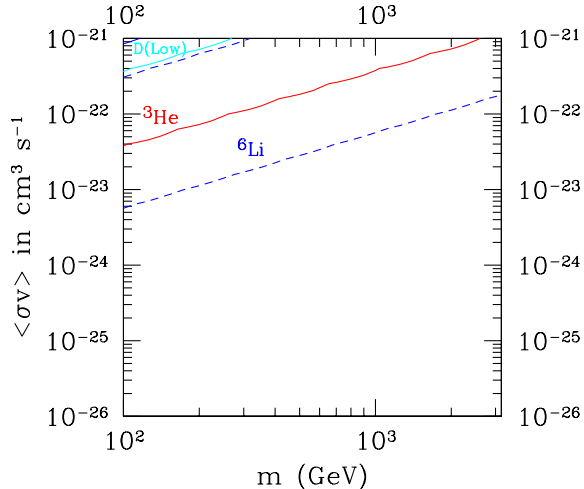


Figure 1: BBN constraints on the annihilation cross section of DM particles when we take $D_7 = 0.35$. The red, cyan, blue, green and brown solid curves represent the upper bounds from observational constraints on ${}^3\text{He}/\text{D}$, D , ${}^6\text{Li}$, ${}^7\text{Li}$ and ${}^4\text{He}$, respectively. The name of the element is also written by each line. As for D , we plot both upper limits from High and Low values. Here we assume that the dark matter annihilates only into e^+e^- , which means the fraction of the visible energy is $E_{\text{vis}}/m = 2$. The lines of ${}^4\text{He}$, ${}^6\text{Li}$ and ${}^7\text{Li}$ do not appear in this figure. For reference, the region sandwiched by two dashed lines is allowed by ${}^6\text{Li}$ when we take $D_7 = 0$.

element abundances predicted from the standard BBN is consistent with the observations, we obtain an upper bound on $\langle\sigma v\rangle$ in order not to spoil the success of the BBN.

In this section, we calculate the abundances of light elements for several different DM scenarios, taking account of non-thermal production processes discussed in the previous section. Then, we compare the theoretical results with observational constraints to derive the upper bound on $\langle\sigma v\rangle$. As we will see below, the constraints on the cross section depend on the dominant annihilation process; if the DM dominantly annihilates into charged leptons and/or photons, the photo-dissociation processes are the most important effect, while the hadronic effects becomes more significant when colored particles are produced by the annihilation. In the following, we consider several typical cases.

3.1 Charged-leptonic modes

The simplest way of explaining the PAMELA and ATIC anomalies is to adopt the possibility that the DM dominantly annihilates into charged lepton pair: $\text{DM} + \text{DM} \rightarrow \ell^+ + \ell^-$. We start with considering such a possibility.

We first show the constraints on $\langle\sigma v\rangle$ for the case where $\text{DM} + \text{DM} \rightarrow e^+ + e^-$ is the dominant annihilation process (Fig. 1). Since $E_{\text{vis}} \propto m_{\text{DM}}$, the constraints depend on $\langle\sigma v\rangle/m_{\text{DM}}$. The most stringent constraint comes from ${}^3\text{He}/\text{D}$.

We can convert the constraints given in Fig. 1 to other cases as far as the effects of hadronic decay modes are negligible; since the effects of the photo-dissociation depend only on E_{vis} , the upper bounds from the photo-dissociation processes scale as E_{vis} . In

particular, if we use the most stringent upper bound, which is from ${}^3\text{He}/\text{D}$, we obtain

$$\langle\sigma v\rangle < 3.5 \times 10^{-22} \text{ cm}^3\text{s}^{-1} \left(\frac{E_{\text{vis}}}{2m_{\text{DM}}}\right)^{-1} \left(\frac{m_{\text{DM}}}{1 \text{ TeV}}\right). \quad (11)$$

For the case where $\text{DM} + \text{DM} \rightarrow \mu^+ + \mu^-$ or $\tau^+ + \tau^-$ is the dominant annihilation process, the constraints can be easily obtained from Fig. 1 by using Eq. (11), because the photo-dissociation effect on BBN is determined by the total visible energy injection by the annihilation process.⁵

For the cases of $\text{DM} + \text{DM} \rightarrow \mu^+ + \mu^-$ and $\tau^+ + \tau^-$, the upper bounds are given by $\langle\sigma v\rangle < 1.0 \times 10^{-21} \text{ cm}^3\text{s}^{-1} \times (m_{\text{DM}}/1 \text{ TeV})^{-1}$ and $1.2 \times 10^{-21} \text{ cm}^3\text{s}^{-1} \times (m_{\text{DM}}/1 \text{ TeV})^{-1}$, respectively.

3.2 Hadronic modes

Next, we consider effects of hadronic modes. Even though we are mainly interested in models which can explain the excess of cosmic-ray e^\pm , it does not necessarily exclude models in which significant amount of hadrons are emitted by the annihilation process.

One of the well-motivated cases is that the annihilation cross section into the W^+W^- pair is sizable. This is the case when, for example, the Wino in the supersymmetric model is the lightest SUSY particle (LSP) and is the DM. As we discuss in the following subsection, the PAMELA and ATIC anomalies may be explained in such a case. Then, importantly, leptonic decay of the produced W^\pm is important for the production of cosmic-ray e^\pm , while the BBN constraint is mainly due to the hadronic decay mode.

In Fig. 2, we show the bound on the annihilation cross section for the case where the DM annihilates only into the W^+W^- pair. For $m_{\text{DM}} \lesssim 2 \text{ TeV}$, as one can see, the D abundance gives the severest constraint on the annihilation cross section if we adopt the low value of the observational D; this is due to the hadro-dissociation process of abundant ${}^4\text{He}$. Then, in such a case, we can obtain an approximate constraint on the annihilation cross section as a function of the mass: $\langle\sigma v\rangle \lesssim 10^{-23} \text{ cm}^3\text{s}^{-1} (N_n/0.8)^{-1} (m_{\text{DM}}/1 \text{ TeV})^{1.5}$, with N_n being the number of emitted neutrons per single annihilation (~ 0.8 in the case of W^+W^- emission); here, we have used the approximate relation discussed in the previous section: $\xi_{A,\text{ann}} \propto m_{\text{DM}}^{0.5}$.

So far, we have considered cases where energetic charged leptons (in particular, e^\pm) are directly produced by the annihilation of the DM or the decay of heavy particle (i.e., W^\pm). Such cases are important to explain the behavior of the e^\pm fluxes observed by the PAMELA and ATIC, because e^\pm produced via the hadronization process is less energetic. Consequently, in the light of PAMELA and ATIC, scenarios where the DM annihilates

⁵ For $T \lesssim \text{keV}$ where the photo-dissociation of ${}^4\text{He}$ is effective, both muon and tau leptons decay well before they lose their initial kinetic energies through scattering off the background photons and electrons. That is because timescales of the Inverse Compton (IC) and the Coulomb scatterings (CS) are given by $t_{\text{IC}} \sim 2.2 \times 10^{-10} \text{ s} (\gamma_{\ell^\pm}/10^3)^{-1} (T/\text{keV})^{-4} (m_{\ell^\pm}/m_e)^3$ and $t_{\text{CS}} \sim 0.76 \times 10^5 \text{ s} (E_{\ell^\pm}/10^2 \text{ GeV}) (T/\text{keV})^{-3}$ with γ_{ℓ^\pm} being the Lorentz factor, m_{ℓ^\pm} the mass, and E_{ℓ^\pm} the energy of charged lepton ℓ^\pm ($= \mu$ and τ), respectively.

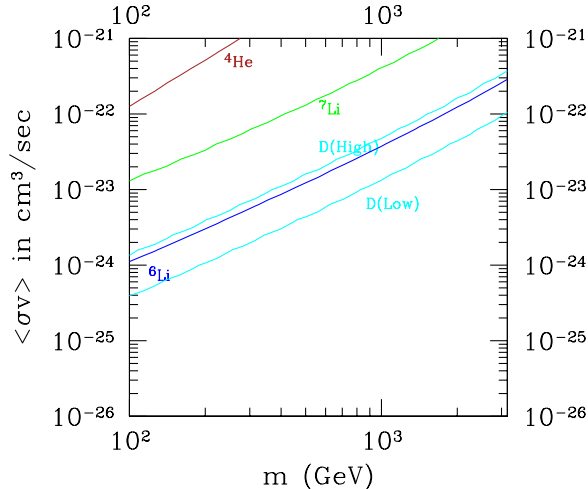


Figure 2: Same as Fig. 1 but for the annihilation into W^+W^- pair. Then the fraction of the visible energy is $E_{\text{vis}}/m = 0.94$.

only into colored particles (like a quark pair or a gluon pair) are less attractive. However, in general, the DM may annihilates dominantly into colored particles. Thus, we also comment on constraints on the annihilation cross section in such a case. Here, as an example, we consider the case where the DM annihilates dominantly into a $b\bar{b}$ pair; the constraints is shown in the top panel of Fig. 3. The fraction of the visible energy is $E_{\text{vis}}/m_{\text{DM}} = 1.04$. In this mode, the number of emitted neutrons is an increasing function of m_{DM} (0.3–0.5 for $m_{\text{DM}} = 100$ GeV–1 TeV). For comparison, we also study the case that $\langle\sigma v\rangle_{\text{DM}+\text{DM}\rightarrow b+\bar{b}}/\langle\sigma v\rangle_{\text{DM}+\text{DM}\rightarrow\text{all}} = 0.01$, with keeping the relation $E_{\text{vis}}/m_{\text{DM}} = 1.04$; the constraints are shown in the bottom panel of Fig. 3. Comparing the top panel with the bottom one, we see that the constraints from the photo-dissociation dominates if the hadronic mode is less than 1 %.

3.3 Implication to PAMELA/ATIC

In previous subsections, we have seen that the quantity $\langle\sigma v\rangle$ should be smaller than $\sim O(10^{-24} - 10^{-21}) \text{ cm}^3\text{s}^{-1}$ in order not to spoil the success of the BBN, if the dominant annihilation process of the DM is into e^+e^- , $\mu^+\mu^-$, $\tau^+\tau^-$, W^+W^- , $b\bar{b}$, and so on. In fact, the upper bound on $\langle\sigma v\rangle$ is of the similar order of that required to explain the PAMELA and ATIC anomalies.

To see this, we plot the positron fraction and the total electron and positron flux in Figs. 4 and 5, respectively. Here, we adopt the background fluxes of electron and positron of Ref. [52]. The annihilation cross section and the DM particle mass (as well the propagation model) used in obtaining Figs. 4 and 5 is summarized in Table 2. In Fig. 4 (Fig. 5), we also show the data points of HEAT [57] and PAMELA [4] (BETS [58], PPB-BETS [59] and ATIC [5]).⁶ From the figures, we can see that DM models with

⁶Recently the HESS collaboration also reported electron flux with $E \gtrsim 600$ GeV [60], which is consis-

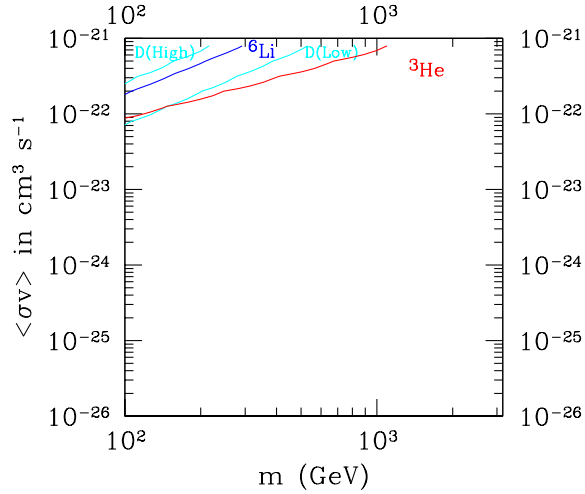
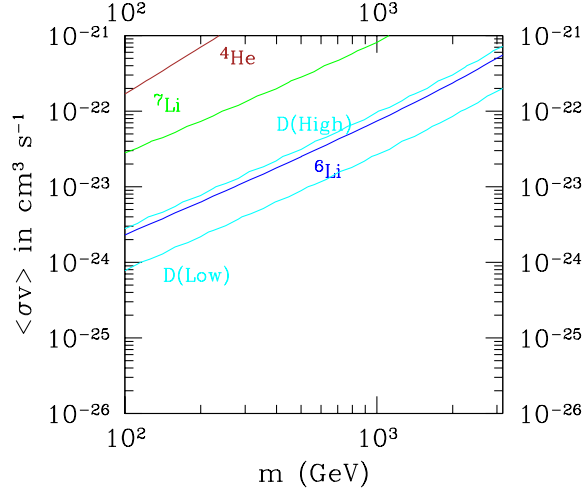


Figure 3: Same as Fig. 1 but for the annihilation into $b\bar{b}$ pair (top panel). Then the fraction of the visible energy is $E_{\text{vis}}/m = 1.04$. For comparison, we also plot the case of $b + \bar{b}$ emission at 1% in the bottom panel virtually by changing the hadronic branching ratio from 1 to 0.01 by hand with keeping the same value of E_{vis} .

the annihilation cross section of $\langle\sigma v\rangle \sim 10^{-23} \text{ cm}^3\text{s}^{-1}$ well explains the anomalies in the cosmic-ray e^\pm fluxes.

To calculate the electron and positron fluxes from the DM annihilation, we have adopted the conventional procedure [53]. Approximating the shape of the diffusion zone as a cylinder (with half-height L and the length $2R = 40 \text{ kpc}$), we have derived the static solution to the following diffusion equation [54]:

$$\frac{\partial}{\partial t}f(E, \vec{x}) = K(E)\nabla^2f(E, \vec{x}) + \frac{\partial}{\partial E}[b(E)f(E, \vec{x})] + Q(E, \vec{x}), \quad (12)$$

where $f(E, \vec{x})$ is the electron/positron number density with energy E at the position \vec{x} , which is related to the DM contribution to the electron and positron fluxes as

$$\Phi_{e^+}^{(\text{DM})}(E, \vec{x}_\odot) = \frac{c}{4\pi}f(E, \vec{x}_\odot), \quad (13)$$

where c is the speed of light and \vec{x}_\odot denotes the position of the solar system. In Eq. (12), $K(E)$ is the diffusion constant, and $Q(E, \vec{x})$ is the source term from the DM annihilation. For the energy loss rate, we use $b(E) = 1 \times 10^{-16}(E/1 \text{ GeV})^2$.

The derived positron and electron fluxes are sensitive to the diffusion constant and the half-height of the diffusion cylinder L . The diffusion constant is parametrized as $K = K_0(E/1 \text{ GeV})^\delta$. Hereafter we consider the following two propagation models, called the MED model: $(K_0, \delta, L) = (0.0112 \text{ kpc}^2/\text{Myr}, 0.70, 4 \text{ kpc})$ and M2 model: $(K_0, \delta, L) = (0.00595 \text{ kpc}^2/\text{Myr}, 0.55, 1 \text{ kpc})$, both of which are consistent with observed boron-to-carbon ratio in the cosmic-ray flux [55].

The source term in Eq. (12) is given by

$$Q(E, \vec{x}) = \frac{1}{2}B_F n_{\text{DM,now}}^2(\vec{x})\langle\sigma v\rangle \left[\frac{dN_{e^\pm}}{dE} \right]_{\text{ann}}, \quad (14)$$

where $n_{\text{DM,now}}(\vec{x})$ is the present DM distribution (in particular, in the halo). Dependence of the electron and positron fluxes on the DM density profile is very minor. In our calculation, we use the isothermal density profile as $\rho_{\text{DM,now}}(r) = m_{\text{DM}}n_{\text{DM,now}}(r) = 0.43(2.8^2 + 8.5^2)/(2.8^2 + r_{\text{kpc}}^2) \text{ GeV cm}^{-3}$, where r_{kpc} is the distance from the Galactic center in units of kpc. Furthermore, according to N -body simulations, the dark matter may not be distributed smoothly in our Galaxy and there may be clumpy structures somewhere in the Galactic halo. If this is the case, the positron flux may be enhanced [56]. In Eq. (14) such an effect is considered by the boost factor B_F .

It is found from the figures that the best-fit values of the DM particle mass and the annihilation cross section to the PAMELA and ATIC observations depend on the annihilation modes. For example, if the DM dominantly annihilates as $\text{DM} + \text{DM} \rightarrow e^+ + e^-$, $m_{\text{DM}} \simeq 650 \text{ GeV}$ and $B_F\langle\sigma v\rangle \simeq 0.5 \times 10^{-23} \text{ cm}^3\text{s}^{-1}$ is preferred to explain the anomalies.⁷ As we have seen in the previous subsection, when $m_{\text{DM}} \simeq 650 \text{ GeV}$, the

tent with ATIC results.

⁷ Model parameters used here and hereafter are just for the representative purpose and the fit to the observational data is still reasonable even if the parameters are varied up to a few ten's of percent. However, the following conclusions are not affected with such changes of parameters.

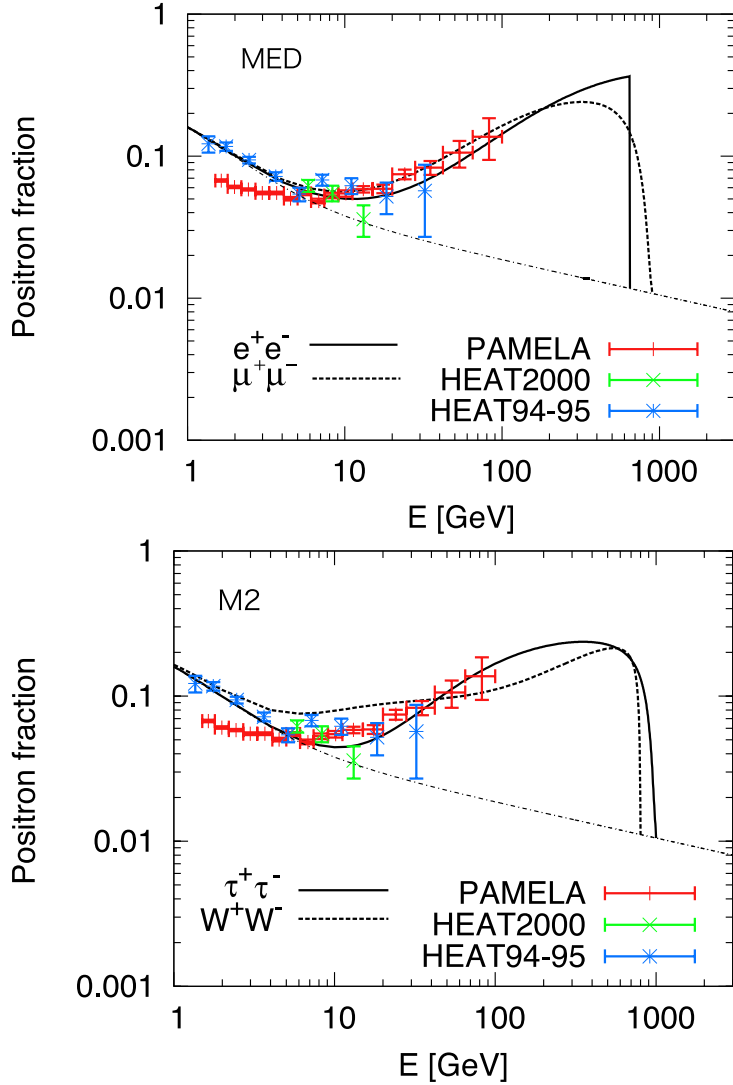


Figure 4: Positron fraction R as a function of positron energy E . (Top) We assume the DM annihilating into e^+e^- with annihilation cross section $\langle\sigma v\rangle = 5 \times 10^{-24} \text{ cm}^3\text{s}^{-1}$ for $m_{\text{DM}} = 650 \text{ GeV}$, and into $\mu^+\mu^-$ with $\langle\sigma v\rangle = 15 \times 10^{-24} \text{ cm}^3\text{s}^{-1}$ for $m_{\text{DM}} = 900 \text{ GeV}$ for the MED propagation model. (Bottom) We assume DM annihilating into $\tau^+\tau^-$ with annihilation cross section $\langle\sigma v\rangle = 4 \times 10^{-23} \text{ cm}^3\text{s}^{-1}$ for $m_{\text{DM}} = 1 \text{ TeV}$, and into W^+W^- with $\langle\sigma v\rangle = 3 \times 10^{-23} \text{ cm}^3\text{s}^{-1}$ for $m_{\text{DM}} = 800 \text{ GeV}$ for the M2 propagation model. Results of PAMELA and HEAT experiments are also shown.

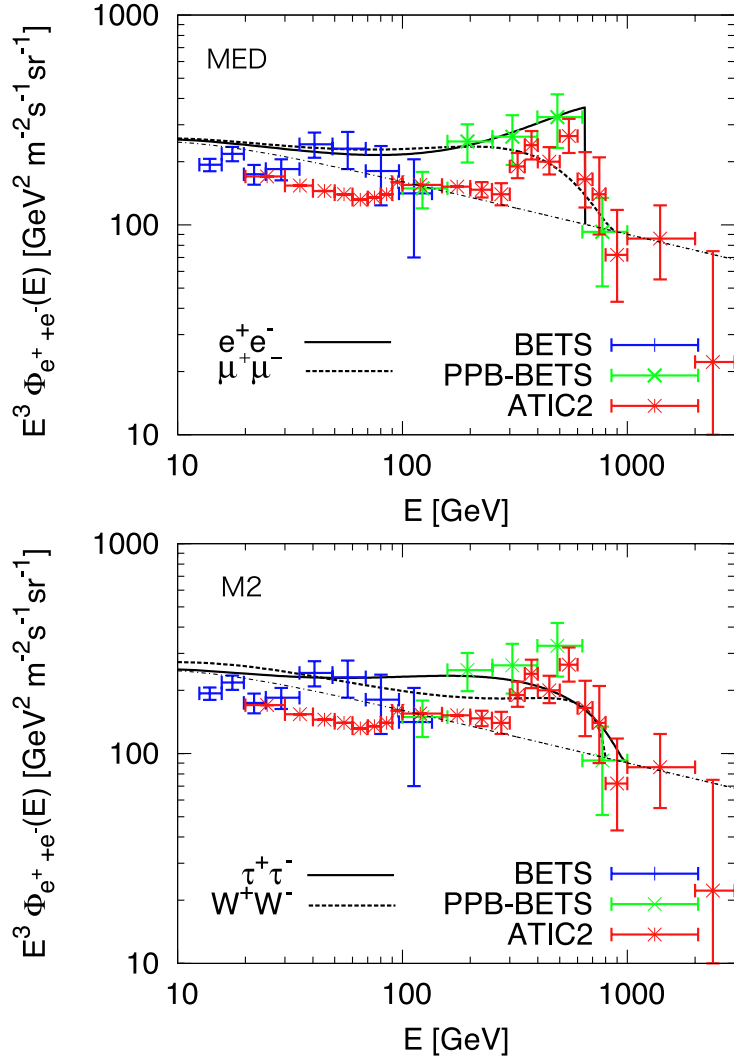


Figure 5: Total electron and positron flux (times E^3) as a function of their energy. Model parameters are same as Fig. 4. Results of BETS, PPB-BETS and ATIC are plotted.

Final State	m_{DM} (GeV)	$B_F \langle \sigma v \rangle$ ($\text{cm}^3 \text{s}^{-1}$)	Propagation Model
e^+e^-	650	0.5×10^{-23}	MED
$\mu^+\mu^-$	900	1.5×10^{-23}	MED
$\tau^+\tau^-$	1000	4.0×10^{-23}	M2
W^+W^-	800	3.0×10^{-23}	M2

Table 2: DM particle mass, the product $B_F \langle \sigma v \rangle$, and the propagation model used in Figs. 4 and 5.

BBN constraint requires $\langle \sigma v \rangle \leq 2.3 \times 10^{-22} \text{ cm}^3 \text{s}^{-1}$, and hence the PAMELA and ATIC anomalies can be explained even if $B_F = 1$. For the case where the DM annihilates as $\text{DM} + \text{DM} \rightarrow W^+ + W^-$, it is remarkable that we need a sizable boost factor (for example, $\gtrsim 4$), because the observations require $\langle \sigma v \rangle = 3 \times 10^{-23} \text{ cm}^3 \text{s}^{-1}$ for $m_{\text{DM}} = 800 \text{ GeV}$ for the M2 propagation model, as shown in Figs. 4 and 5.

4 Conclusions and Discussion

In this paper we have investigated the effect of the DM annihilation on BBN. Recent observations of the cosmic-ray positron/electron excess by the PAMELA/ATIC experiments can be interpreted as the contribution from the DM annihilation. However, this requires very large annihilation cross section as $\langle \sigma v \rangle \sim 10^{-23} \text{ cm}^3 \text{s}^{-1}$ unless the boost factor is not introduced, and such large annihilation rate can have significant effects on BBN.

We found that leptonically annihilating DM models are constrained from the upper bound on ${}^3\text{He}/\text{D}$. This limit is compatible with the DM annihilation models for explaining the PAMELA and ATIC anomalies for the case of annihilation into e^+e^- , $\mu^+\mu^-$ and $\tau^+\tau^-$. On the other hand, the DM annihilation models with significant amount of hadrons are constrained from the observations of D or ${}^6\text{Li}$ abundances. This gives a stringent constraint in some case; the DM models annihilating into W -bosons for explaining both the PAMELA and ATIC anomalies are excluded unless the boost factor larger than unity is introduced.

In this paper we assumed that the DM annihilation cross section is independent of the cosmic time. However, our results also have impacts on scenarios with the time-dependent cross section. When the DM annihilates through a pole just below the threshold, the annihilation cross section is enhanced for lower relative velocity of the annihilating DM particles [17]. This enhancement is automatically implemented in the Sommerfeld mechanism [7, 61]. Then, the large boost factor may not be required to realize both the thermal freezeout scenario of the DM and the enhanced e^\pm fluxes consistent with the PAMELA/ATIC. However, in such scenarios, it is notable that the annihilation cross section during the BBN epoch may be significantly enhanced than that in the present Galaxy. Since our results indicate that the DM annihilation cross section in the BBN epoch cannot be much larger than that in the Galaxy now, those models are excluded if

the enhancement of the cross section during the BBN epoch is sizable.

Some comments are in order. The DM annihilation in the Galactic center yields significant amount of gamma-rays through the cascade decay of the annihilation products and/or bremsstrahlung processes, which must be compared with the HESS observation [62]. However, the gamma-ray flux significantly depends on the DM density profile, and if a moderate profile such as an isothermal one with rather large core radius [63] is chosen, the constraint is loosen [11].

DM annihilation cross section can also be constrained from the observations of anti-protons [64, 65] in the case of hadronic annihilation mode, and synchrotron radiation [11, 66] produced by the DM annihilation inside the Galaxy. However, these constraints more or less suffer from astrophysical uncertainties, such as the density profile of the DM halo, the size of the diffusion zone and the distribution of the magnetic field. They lead to orders of magnitude uncertainties on the resulting constraints [67, 68]. Taking into account these uncertainties, DM annihilation models are consistent with observations [65, 11].

Neutrinos from the DM annihilation at the Galactic center [12] (and possibly from the DM trapped inside the Earth [69]) may also be useful as a tool for cross-checking signatures of DM annihilation and Super-Kamiokande [70] gives constraints on some DM annihilation models. However, it still depends on the DM density profile, though the dependence is rather weak.

The constraints on the DM annihilation cross section from BBN presented in this paper is robust, since they do not suffer from large astrophysical uncertainties, compared with those DM signatures in the cosmic rays.

Acknowledgment

K.N. would like to thank the Japan Society for the Promotion of Science for financial support. This work is supported by Grant-in-Aid for Scientific research from the Ministry of Education, Science, Sports, and Culture (MEXT), Japan, No. 20244037, No. 2054252 (J.H.), No. 14102004 (M.K.) and No. 19540255 (T.M.), and also by World Premier International Research Center Initiative, MEXT, Japan. K.K. is supported in part by STFC grant, PP/D000394/1, EU grant MRTN-CT-2006-035863, the European Union through the Marie Curie Research and Training Network “UniverseNet.”

References

- [1] E. Komatsu *et al.* [WMAP Collaboration], arXiv:0803.0547 [astro-ph].
- [2] G. Jungman, M. Kamionkowski and K. Griest, Phys. Rept. **267**, 195 (1996).
- [3] G. Bertone, D. Hooper and J. Silk, Phys. Rept. **405**, 279 (2005).
- [4] O. Adriani *et al.*, arXiv:0810.4995 [astro-ph].

- [5] J. Chang *et al.*, Nature **456**, 362 (2008).
- [6] L. Bergstrom, T. Bringmann and J. Edsjo, arXiv:0808.3725 [astro-ph]; V. Barger, W. Y. Keung, D. Marfatia and G. Shaughnessy, arXiv:0809.0162 [hep-ph]; M. Cirelli, M. Kadastik, M. Raidal and A. Strumia, arXiv:0809.2409 [hep-ph]; I. Cholis, D. P. Finkbeiner, L. Goodenough and N. Weiner, arXiv:0810.5344 [astro-ph]; Y. Nomura and J. Thaler, arXiv:0810.5397 [hep-ph]; D. Feldman, Z. Liu and P. Nath, arXiv:0810.5762 [hep-ph]; K. Ishiwata, S. Matsumoto and T. Moroi, arXiv:0811.0250 [hep-ph]; P. J. Fox and E. Poppitz, arXiv:0811.0399 [hep-ph].
- [7] J. Hisano, S. Matsumoto and M. M. Nojiri, Phys. Rev. Lett. **92**, 031303 (2004); J. Hisano, S. Matsumoto, M. M. Nojiri and O. Saito, Phys. Rev. D **71**, 063528 (2005).
- [8] M. Kawasaki, T. Moroi and T. Yanagida, Phys. Lett. B **370**, 52 (1996).
- [9] T. Moroi and L. Randall, Nucl. Phys. B **570**, 455 (2000); M. Fujii and K. Hamaguchi, Phys. Lett. B **525**, 143 (2002); Phys. Rev. D **66**, 083501 (2002); M. Nagai and K. Nakayama, Phys. Rev. D **76**, 123501 (2007); B. S. Acharya, P. Kumar, K. Bobkov, G. Kane, J. Shao and S. Watson, arXiv:0804.0863 [hep-ph].
- [10] S. Profumo and P. Ullio, JCAP **0407**, 006 (2004); M. Nagai and K. Nakayama, Phys. Rev. D **78**, 063540 (2008); P. Grajek, G. Kane, D. J. Phalen, A. Pierce and S. Watson, arXiv:0807.1508 [hep-ph].
- [11] G. Bertone, M. Cirelli, A. Strumia and M. Taoso, arXiv:0811.3744 [astro-ph].
- [12] J. Hisano, M. Kawasaki, K. Kohri and K. Nakayama, arXiv:0812.0219 [hep-ph]; J. Liu, P. f. Yin and S. h. Zhu, arXiv:0812.0964 [astro-ph].
- [13] K. Jedamzik, Phys. Rev. D **70**, 083510 (2004).
- [14] M. H. Reno and D. Seckel, Phys. Rev. D **37**, 3441 (1988).
- [15] J. A. Frieman, E. W. Kolb and M. S. Turner, Phys. Rev. D **41**, 3080 (1990).
- [16] J. Hisano, M. Kawasaki, K. Kohri and K. Nakayama, arXiv:0810.1892 [hep-ph].
- [17] M. Ibe, H. Murayama and T. T. Yanagida, arXiv:0812.0072 [hep-ph].
- [18] T. Sjostrand, S. Mrenna and P. Skands, JHEP **0605**, 026 (2006).
- [19] J. R. Ellis *et al.*, Nucl. Phys. B **373**, 399 (1992); M. Kawasaki and T. Moroi, Prog. Theor. Phys. **93**, 879 (1995); E. Holtmann, M. Kawasaki, K. Kohri and T. Moroi, Phys. Rev. D **60**, 023506 (1999); K. Jedamzik, Phys. Rev. Lett. **84**, 3248 (2000); M. Kawasaki, K. Kohri and T. Moroi, Phys. Rev. D **63**, 103502 (2001); R. H. Cyburt, J. R. Ellis, B. D. Fields and K. A. Olive, Phys. Rev. D **67**, 103521 (2003). J. R. Ellis, K. A. Olive and E. Vangioni, Phys. Lett. B **619**, 30 (2005).

- [20] M. Kawasaki and T. Moroi, *Astrophys. J.* **452**, 506 (1995).
- [21] M. S. Smith, L. H. Kawano and R. A. Malaney, *Astrophys. J. Suppl.* **85**, 219 (1993).
- [22] C. Angulo *et al.*, *Nucl. Phys. A* **656**, 3 (1999).
- [23] R. H. Cyburt, B. D. Fields and K. A. Olive, *New Astron.* **6**, 215 (2001); R. H. Cyburt, *Phys. Rev. D* **70**, 023505 (2004).
- [24] P. D. Serpico, S. Esposito, F. Iocco, G. Mangano, G. Miele and O. Pisanti, *JCAP* **0412**, 010 (2004).
- [25] R. H. Cyburt and B. Davids, arXiv:0809.3240 [nucl-ex].
- [26] L. M. Krauss and P. Romanelli, *Astrophys. J.*, 338 (1990) 47.
- [27] K. Jedamzik, *Phys. Rev. D* **70**, 063524 (2004).
- [28] M. Kawasaki, K. Kohri and T. Moroi, *Phys. Lett. B* **625**, 7 (2005).
- [29] M. Kawasaki, K. Kohri and T. Moroi, *Phys. Rev. D* **71**, 083502 (2005).
- [30] M. Kawasaki, K. Kohri, T. Moroi and A. Yotsuyanagi, arXiv:0804.3745 [hep-ph].
- [31] K. Jedamzik, *Phys. Rev. D* **74**, 103509 (2006).
- [32] K. Kohri, *Phys. Rev. D* **64**, 043515 (2001).
- [33] J. M. O'Meara *et al.*, *Astrophys. J.* **649**, L61 (2006).
- [34] G. Sigl, K. Jedamzik, D. N. Schramm and V. S. Berezinsky, *Phys. Rev. D* **52**, 6682 (1995).
- [35] J. Geiss and G. Gloeckler, *Space Science Reviews* **106**, 3 (2003).
- [36] Y. I. Izotov, T. X. Thuan and G. Stasinska, arXiv:astro-ph/0702072.
- [37] M. Fukugita and M. Kawasaki, *Astrophys. J.* **646**, 691 (2006).
- [38] M. Peimbert, V. Luridiana and A. Peimbert, arXiv:astro-ph/0701580.
- [39] P. Bonifacio *et al.*, arXiv:astro-ph/0610245.
- [40] S.G. Ryan *et al.*, *Astrophys. J. Lett.* **530**, L57 (2000).
- [41] J. Melendez and I. Ramirez, *Astrophys. J.* **615**, L33 (2004).
- [42] R. H. Cyburt, B. D. Fields and K. A. Olive, arXiv:0808.2818 [astro-ph].
- [43] M. Asplund *et al.*, *Astrophys. J.* **644**, 229 (2006).

- [44] M. H. Pinsonneault, G. Steigman, T. P. Walker and V. K. Narayanan, *Astrophys. J.* **574**, 398 (2002).
- [45] A. J. Korn *et al.*, *Nature* **442**, 657 (2006); A. J. Korn *et al.*, *Astrophys. J.* **671**, 402 (2007).
- [46] A. Coc *et al.*, *Astrophys. J.* **600**, 544 (2004); C. Angulo *et al.*, *Astrophys. J.* **630**, L105 (2005).
- [47] K. Ichikawa and M. Kawasaki, *Phys. Rev. D* **69**, 123506 (2004); K. Ichikawa, M. Kawasaki and F. Takahashi, *Phys. Lett. B* **597**, 1 (2004); K. Kohri, T. Moroi and A. Yotsuyanagi, *Phys. Rev. D* **73**, 123511 (2006); K. Jedamzik, K. Y. Choi, L. Roszkowski and R. Ruiz de Austri, *JCAP* **0607**, 007 (2006). K. Kohri and F. Takayama, *Phys. Rev. D* **76**, 063507 (2007); R. H. Cyburt *et al.*, *JCAP* **0611**, 014 (2006); K. Jedamzik, arXiv:0707.2070 [astro-ph]; K. Jedamzik, arXiv:0710.5153 [hep-ph]; C. Bird, K. Koopmans and M. Pospelov, arXiv:hep-ph/0703096; T. Jittoh *et al.*, *Phys. Rev. D* **76**, 125023 (2007); *Phys. Rev. D* **78**, 055007 (2008); D. Cumberbatch *et al.*, *Phys. Rev. D* **76**, 123005 (2007); M. Kusakabe *et al.*, *Phys. Rev. D* **76**, 121302 (2007); arXiv:0711.3858 [astro-ph]; K. Kohri and Y. Santoso, arXiv:0811.1119 [hep-ph].
- [48] T. K. Suzuki and S. Inoue, *Astrophys. J.* **573**, 168 (2002); E. Rollinde, E. Vangioni and K. A. Olive, *Astrophys. J.* **651**, 658 (2006); V. Tatischeff and J. P. Thibaud; *Astron. and Astrophys.* in press [arXiv:astro-ph/0610756]. E. Rollinde, D. Maurin, E. Vangioni, K. A. Olive and S. Inoue, arXiv:0707.2086 [astro-ph]; K. Nakamura and T. Shigeyama, *Astrophys. J.* **610**, 888 (2004); K. Nakamura and T. Shigeyama, *Astrophys. J.* **645**, 431 (2006).
- [49] R. Cayrel *et al.*, arXiv:0708.3819 [astro-ph]; R. Cayrel, M. Steffen, P. Bonifacio, H. G. Ludwig and E. Caffau, arXiv:0810.4290 [astro-ph].
- [50] T. Kanzaki, M. Kawasaki, K. Kohri and T. Moroi, *Phys. Rev. D* **75**, 025011 (2007).
- [51] M. H. Pinsonneault, T. P. Walker, G. Steigman and V. K. Narayanan, *Astrophys. J.* **527**, 180 (1999).
- [52] I. V. Moskalenko and A. W. Strong, *Astrophys. J.* **493**, 694 (1998).
- [53] J. Hisano, S. Matsumoto, O. Saito and M. Senami, *Phys. Rev. D* **73**, 055004 (2006).
- [54] E. A. Baltz and J. Edsjo, *Phys. Rev. D* **59**, 023511 (1999).
- [55] T. Delahaye, R. Lineros, F. Donato, N. Fornengo and P. Salati, *Phys. Rev. D* **77**, 063527 (2008).
- [56] J. Silk and A. Stebbins, *Astrophys. J.* **411**, 439 (1993); L. Bergstrom, J. Edsjo, P. Gondolo and P. Ullio, *Phys. Rev. D* **59**, 043506 (1999).

- [57] S. W. Barwick *et al.* [HEAT Collaboration], *Astrophys. J.* **482**, L191 (1997);
J. J. Beatty *et al.*, *Phys. Rev. Lett.* **93**, 241102 (2004).
- [58] S. Torii *et al.*, *Astrophys. J.* **559**, 973 (2001).
- [59] S. Torii *et al.*, arXiv:0809.0760 [astro-ph].
- [60] H. E. S. S. Collaboration, arXiv:0811.3894 [astro-ph].
- [61] J. Hisano, S. Matsumoto, M. Nagai, O. Saito and M. Senami, *Phys. Lett. B* **646**, 34 (2007) [arXiv:hep-ph/0610249].
- [62] F. Aharonian *et al.* [The HESS Collaboration], *Astron. Astrophys.* **425**, L13 (2004);
F. Aharonian *et al.* [H.E.S.S. Collaboration], *Phys. Rev. Lett.* **97**, 221102 (2006)
[Erratum-ibid. **97**, 249901 (2006)].
- [63] P. Salucci, A. Burkert, *Astrophys. J.* **537**, L9 (2000); P. Salucci, A. Lapi, C. Tonini,
G. Gentile, I. Yegorova, U. Klein, *MNRAS*, **378**, 41 (2007).
- [64] F. Donato, D. Maurin, P. Brun, T. Delahaye and P. Salati, arXiv:0810.5292 [astro-ph].
- [65] P. Grajek, G. Kane, D. Phalen, A. Pierce and S. Watson, arXiv:0812.4555 [hep-ph].
- [66] J. Zhang, X. J. Bi, J. Liu, S. M. Liu, P. f. Yin, Q. Yuan and S. H. Zhu,
arXiv:0812.0522 [astro-ph]; L. Bergstrom, G. Bertone, T. Bringmann, J. Edsjo and
M. Taoso, arXiv:0812.3895 [astro-ph].
- [67] F. Donato, N. Fornengo, D. Maurin and P. Salati, *Phys. Rev. D* **69**, 063501 (2004).
- [68] E. Borriello, A. Cuoco and G. Miele, arXiv:0809.2990 [astro-ph].
- [69] C. Delaunay, P. J. Fox and G. Perez, arXiv:0812.3331 [hep-ph].
- [70] S. Desai *et al.* [Super-Kamiokande Collaboration], *Phys. Rev. D* **70**, 083523 (2004)
[Erratum-ibid. D **70**, 109901 (2004)]; *Astropart. Phys.* **29**, 42 (2008).